JETIR.ORG ISSN: 2349-5162 | ESTD Year : 2014 | Monthly Issue
JOURNAL OF EMERGING TECHNOLOGIES AND INNOVATIVE RESEARCH (JETIR)
An International Scholarly Open Access, Peer-reviewed, Refereed Journal

Integrated Quality by Design Strategy for the Development of TPGS-Loaded Liposomal Formulations Targeting Antimicrobial Resistance

Jahnvi Srivastava*, Santoshi shah, Dr. Shrivanand patil

Department of Quality Assurance, Shri dev Bhoomi institute of education science & technology, Pondha Rd, Majhaun, Uttarakhand 248007.India

ABSTRACT:

Objective:

Irresistible bacterial infectious diseases pose a serious threat to human health, and social workers' failure to act to prevent infections may encourage epidemics and the quick spread of infections among the majority of people. That the need for develop the different approach or method to enhance effect of rifampicin as anti-microbial and reduce the bacterial effect with use liposome and TPGS.

Material method:

A thin film approach was used to generate RIF-LIPO and RIF-LIPO-TPGS, were dissolved in a small volume of a 3:1 v/v methanol and chloroform combination. Rota evaporator used solvent evaporation under vacuum to cast the lipid layer on the inner surface of the flask centrifuge with 15 min. at 3000 rpm. And identification of rifampicin TPGS liposomes with the help of UV, FTIR analysis, XRD, entrapment efficiency. Main target to check the anti-microbial resistance of rifampicin loaded liposome with TPGS. That had already been pre-treated. The formulations placed inside the barrier array were placed in a 37°C-controlled release medium. At intervals of 1, 2, 4, 8, 12, 24, 48, and 72 hours, aliquots of the samples (1.0 mL) were taken out and the same volume (1.0 mL) of new release medium was added to maintain the sink condition.

Result:

FTIR of drug excipients interaction and liposomal formulation depicts no chemical incompatibility were taken place, as no significant change in the vibrational frequency of Rifampicin (RIF) in liposomes were observed.At their respective MICs (1.56 g/ml, 1.56 g/ml, and 1.56 g/m.), Control, Rifampicin, Rifampicin -liposome, and Rifampicin -TPGS- liposome displayed 1244, 1253, 1295, and 27228. demonstrating the superiority of the Rifampicin -TPGS- liposome in terms of enhancing the antibacterial activity of free Rifampicin and Rifampicin -liposome.

Utilizing a dialysis approach, we studied RIF releases kinetics in PBS as a diffusion fluid around 37.1°C to try to decipher that in-vitro RIF releasing behavior from RIF-LIPO and RIF-TPGS-LIPO vesicles. Over the course of 72 hours, the amount of release of liposomes packed by Rifampicin or liposomes that used It TPGS, or was investigated. Rifampicin TPGS liposomes demonstrated about 56+2.7% of the medication release in 72 hours, while more than 73+2.5% of Rifampicin was released in that time

KEYWORDS: quality by Design (QbD); drug delivery; liposomes; nano-pharmaceuticals; nanomedicine.

1. INTRODUCTION:

Currently, one of the biggest threats to public health is antimicrobial resistance (AMR). It happens when bacteria, viruses, fungus, and parasites—among other microorganisms—evolve to withstand the effects of drugs that used to be successfμlin treating the diseases they caused(Dadgostar, 2019). Because of this resistance, normal therapies are no longer effective, which raises the risk of serious sickness and death as well as increased disease transmission and chronic infections.(Majumder et al., 2020)

Numerous reasons contribute to the growth of antimicrobial resistance (AMR), such as the abuse and misuse of antibiotics in both humans and animals(Ventola, 2015), poor strategies for preventing and controlling infections, unsanitary settings, and a lack of quick diagnostics.(Cegielski et al., 2021) Beyond only affecting an individual's health, antimicrobial resistance (AMR) strains healthcare systems worldwide and creates substantial financial costs because of higher mortality, lengthier hospital stays, and other expensive treatment requirements.(Morel et al., 2020)

A multipronged strategy is needed to combat antimicrobial resistance, including enhanced surveillance(Uchil et al., 2014), the creation of novel medicines and alternative treatments, strict management and stewardship of already available antimicrobial drugs, and intensive public awareness campaigns.(Ranjalkar & Chandy, 2019) Through comprehending the workings and causes of antimicrobial resistance (AMR) and putting coordinated local, national, and worldwide initiatives into action, we may counteract this escalating danger and preserve the efficacy of antibiotics for coming generations.(Salam et al., 2023)

2. MATERIAL METHOD:

2.1. Preformulation studies:

Before putting a medicine into a formulation, preformulation studies are a crucial technique for determining its physical and chemical properties(Jones, 2018). The drug's physiochemical characteristics have an essential effect on processing factors such as preparation technique, entrapment effectiveness, compatibility, and in vitro responsiveness of the formulation. Preformulation studies are a crucial step in the process of creating a stable, secure, and safe dose type.(Bhalani et al., 2022)

2.2. Physical characteristics of Rifampicin

Visual observations of physical characteristics such molecular state, colour, and scent were made.(Tang et al., 2023)

2.3. FT-IR spectroscopy

To determine Rifampicin's chemical linkages, FTIR was employed. Rifampicin's spectral range was recorded between 4000 and 400 cm' (Cao et al., 2014)

2.4. UV-Vis spectroscopy

Using a UV-visible spectrophotometer & methanol, a known concentration for Rifampicin (1g/ml) was examined at 400 to 800 nm in order to determine its peak absorption & prepare a standard curve.(Lai et al., 1994)

2.5. Partition coefficient determination

The ratio of a drug's unionised distribution between its aqueous and organic phases at equilibrium is known as the partition coefficient. The partition coefficient of Rifampicin was determined by shake flask method at room temperature using n-octanol: water system.(Maha & AS, 2020)

$$\text{Pow.} = \text{Concentration in organic phase}/\text{Concentration in aqueous phase}$$

$$\text{Log Po/w} = \log (\text{Solute}_{\text{octanol}}/\text{Solute}_{\text{water}})$$

2.6. Melting Point

Measuring approximately 5 cm in length and having a uniform diameter. The drug was then made to fall to the closed end by inverting the capillary tube and giving it a little tap on the counter.(Chooi et al., 2016)

3. Formulation and development of liposomes

3.1. Preparation of RIF-TPGS-Liposomes

A thin film approach was used to generate RIF-LIPO and RIF-LIPO-TPGS, PC or TPGS, CHOL, RIF were dissolved in a small volume of a 3:1 v/v methanol and chloroform combination. Rota evaporator used solvent evaporation under vacuum to cast the lipid layer on the inner surface of the flask, Thin layer was hydrated with the Phosphate buffer (pH 7.2) solution and sonicated with bath sonicator to reduce vesicle size for 20 minutes for the further proceedings (PCi TM analytics). After being sonicated, formulation-created liposomes were three times processed with 0.22 pore size polyether-sulfone filter syringes (Himedia). Using Sephadex-G-50 mini-column centrifugation (3000 rpm for 15 min; Remi, C-24), free RIF was obtained in liposomal mixture in order to determine the proportion of EE. Using lyophilization (Labconco, USA), the final formulations were stored in darkness and a low temperature(Zhu et al., 2013)

3.2. Characterization and evaluation of liposomes

3.2.1. Vesicle Size, PDI, and Surface Morphology

Using a particle size & zeta analyzer (zeta sizer, Backman Coulter), the formulations of (RIF-LIPO & RIF-LIPO-TPGS) were assessed for their average particle size, zeta potential, & polydispersity ratio (PDI). Each experiment was run three times at a 90° angle. Transmission electron microscopy (TEM) (TECNAI 200 Kv TEM, Fei, Electron Optics) was applied to examine the surface structure of the formulation. A metal lattice coated in carbon was used to shield the sample and facilitate imaging. To dye the material negative, 1% of phosphotungstic acid was next used.(Musielak et al., 2022)

3.2.2. Differential Scanning Calorimetric (DSC) analysis

Differential scanning calorimetry (DSC) was performed using a DSC 6000, PerkinElmer, that was calibrated with indium. Common aluminium pans were sealed with three to five milligrams of PC, CHOL, RIF, TPGS, RIF-LIPO, and RIF-LIPO-TPGS for analysis. Here, Aluminum pans that were left empty served as a guide. Thermograms were generated using a scanning range of 30 to 300°C & a scan rate of 20°C/min. Cycle threshold was the term originally used to mean the highest extra warmth of samples.(Gill et al., 2010)

3.2.3. X-ray diffraction (XRD) Analysis

To assess the crystalline pattern of the material, X-ray diffraction (XRD) examination was performed using the Petro, Analytical Netherlands with 2Theta (Coupled Two Theta/Theta) WL-1, 54060 operating at room temperature. The crystalline state of the drug plays a crucial role in drug delivery systems such nanoparticles, microspheres, liposomes, etc. owing to the likelihood that the drug's state will change when it is included in the system. Determining the crystalline nature is important since it influences the drug's release characteristics as well. With the use of the X-ray powder diffraction method (XRD), the drug's solid-state characteristics are investigated. Powder X-ray diffractometer was used to examine RIF-LIPO and RIF-TPGS-LIPO X-ray diffraction patterns. XRD is also used to research how drugs interact with their excipients.

3.2.4. Entrapment Efficiency Determination

Applying previous published techniques, entrapment efficiency (RIF) was obtained(Kurmi & Paliwal, 2022) In summary, a liposome dispersion's 0.2 mL for free RIF was isolated using centrifugation, as previously described, and PBS (pH 7.4) emerged via a Sephadex G-50 mini-column. The UV spectrophotometer (UV-1900, Shimadzu) was used to measure the absorption, the solution at a max wavelength, 337 mm as the sacs were damaged by Triton X-100. To calculate a percentage of EE, the whole amount of drug used in liposome production (RIF-LIPO and RIF-LIPO-TPGS) and the number of drugs that's fully encased are used.(Jain & Shastri, 2011)

3.2.5. Drug Release Analysis

Using a dialysis membrane approach, all formulation' in vitro RIF releasing pattern was assessed on a release medium equal a buffer liquid pH 7.4. RIF-LIPO & RIF-LIPO-TPGS, two distinct 1.0 mL liposomal dispersions, were added to the dialysis membrane bags (MWCO 14 kD; Himedia, LA-395) that had already been pre-treated. The formulations placed inside the barrier array were placed in a 37°C-controlled release medium. At intervals of 1, 2, 4, 8, 12, 24, 48, and 72 hours, aliquots of the samples (1.0 mL) were taken out and the same volume (1.0 mL) of new release medium was added to maintain the sink condition. To determine the RIF concentration, aliquots of the removed samples were exposed to UV light at a maximum wavelength of 337 mm using a UV-Vis spectrometer (UV-1900, Shimadzu).(Gao et al., 2013)

3.2.6. Minimum Inhibitory Concentration (MIC)

Using Mueller-Hinton Broth, the MIC was calculated using the microdilution method. To obtain concentrations ranging from 0.025 to 50 g/ml, the formulations RIF, RIP-LIPO, and RIF-TPGS-LIPO were added to 96-well microplates and serially diluted. Three to five S. aureus colonies were disseminated into a saline solution from 18 to 24 hour agar cultures, and the bacterial inoculum was adjusted using a spectrophotometer (337 mm, OD 0.1, 1 to 2x10? CFU/ml). When the inoculum had been diluted to a final concentration of 5x104 CFU/ml, it was added to the wells. The absorbance was measured at 337 nm after the plates had been incubated for 24 hours at 37 °C. The lowest formulation concentration that prevented discernible bacterial growth was called the MIC. Three duplicates of the experiment were run.(Lee et al., 2007)

3.2.7. ROS detection by flow cytometry

Intracellular ROS production is investigated using 2', 7'-Dichlorofluorescin diacetate (DCFDA). The highly fluorescent chemical 2', 7'-dichlorofluorescein (DCF) is produced by oxidizing DCFDA, a cell-permeable, intracellularly de-esterified non-fluorescent probe. Following plating on a 6-well plate, MDA-MB-231 cells were cultured at 37°C with 5% CO2 for a day with free RIF, RIF-LIPO, and RIF-TPGS-LIPO at scheduled periods. (Sun et al., 2017) After that, the cells were given a PBS wash and allowed to sit in PBS containing 5 uM of DCFDA for half an hour. Following another PBS wash, cells were put back in 500 µlof the solution. When the H2DCF-DA interacting with ROS, it transformed to DCF, which was found and analyzed by FACS. To record DCF info, the excitation wavelength of 488 nm & a reflection frequency at 337 nm was applied. (Singh et al., 2019).

3.2.8. Cell viability by flow cytometry

The flow cytometry assay method was used to conduct investigations on the viability of bacterial cells. The MRSA suspension was made according to the prior instructions at a final concentration of 5x10.. CFU/ml. MIC-equivalent preparations of free RIF (1.56 p/ml), RIF-LIPO (1.56 /ml), and RIF-TPGS-LIPO (1.56 /ml) were made. MRSA (15 ul) was incorporated into a solution in a 96-well plate and incubated at 37°C for 6 hours while being shaken (100 rm) in the incubator. MRSA cells that had not been treated were utilised as a negative control, and following incubation, the percentage of cell viability was calculated. 350 µlof the sheath fluid were combined with 50 µl of raw RIF, RIF-LIPO, and RIF-TPGS-LIPO in separate flow cytometry tubes for each sample, and vortexed for 5 minutes. The mixture was incubated with 5 µl of the non-cell wall permeant Propidium iodide (PI) dye for 30 minutes at 37 °C. A 455 m laser was used to excite PI fluorescence, which was then captured by a 636 nm bandpass filter. The BD Accuri FACS apparatus was used for the flow cytometry study, and the sample and sheath fluid flow rates were set to 16 ml/min and 0.1 ml/min, respectively.(Walvekar et al., 2019).

4. RESULT:

4.1. Pre-formulation study

4.1.1. Physical characteristics of Rifampicin

Rifampicin was characterized for its identity, physical state, color and odor (Table4.1) with respective density 1.3 g/cm', vapor pressure 3.1x10-34mmg (at 25°C) and pH 7.4

Table no.4.1 Physical characterization of rifampicin

Characteristics	Specification	Result
Description	Solid state	Complies
Color	Red brown	Complies
Odor	Odorless	Complies

4.1.2. Melting Point

To determine the quality of Rifampicin, the wizard's capillaries boiling technique was utilized for its melting test. Rifampicin's melting point was determined to be 183–185°C, which agrees with the norm of 182-185°C as indicated in table 4.2.

Table no 4.2 Melting point determination

Test	Standard
183-185ºC	182-185ºC

4.2. Physiochemical Characterization

4.2.1. Vesicle size, PDI and entrapment efficiency determination

Vesicle size and polydispersity index were determined by using Zetasizer. For Rifampicin loaded liposomes, size was found to be 190.5m and PDI was found to be 0.233 is shown in figure 4.1. Furthermore, the entrapment efficiency of the formulation has found to be approx. 87.16%. The high entrapment efficiency of RIP-TPGS-LIPO was ascribed to the loading of RIF and presence of* TPGS on the lipid bilayer of liposomes. The optimized formulation was listed in table 4.3

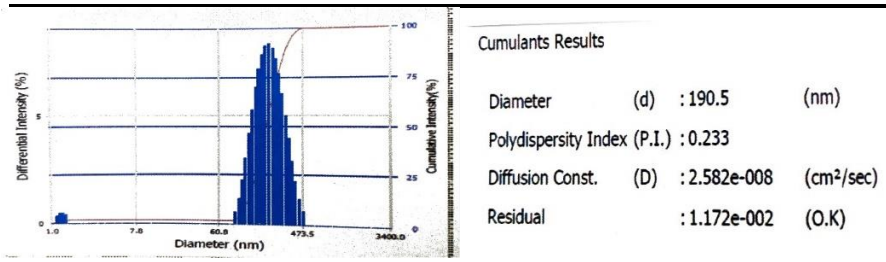

Figure 4.1 Size distribution graph of optimized RIF-TPGS-LIPO

Table no 4.3 Characterization of the developed formulation (mean ± SD, n=3)

Formulation	PDI	Vesicle size (nm)	% EE
RIF-TPGS-LIPO	0.233 ± 0.002	190.5 ± 5.4	87.16% ± 2.8

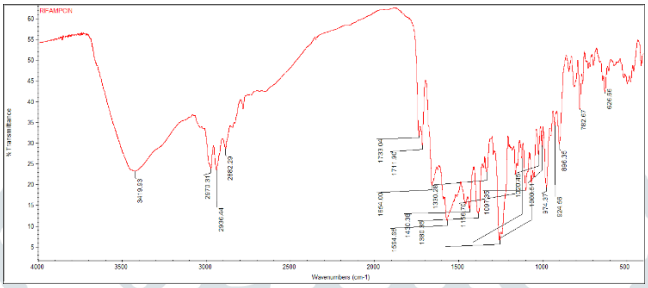

Figure 4.2FTIR Spectra of Rifampicin

Table no.4.4. FITR reading of Rifampicin

Functional group	**Standard wave no. (cm^{-1})**	**Observational wave no. (cm^{-1})**
C=N stretching	1650-1550	1654.00
C=O Acetyl stretching	1725-1700	1711.90
O-H stretching	3500-3350	3419.93
C-H stretching	3100-3000	2936.44
NH stretching	3000-2800	2970.31

4.2.2. Calibration Curve of Rifampicin

The absorbance of the prepared dilutions was observed using UV-visible spectrophotometer at wavelength of 337 nm as shown in table 4.4 Linearity was found between 2 and 20 g/ml as shown in figure 4.3. When the calibration curve was plotted between absorbance and concentrations of rifampicin and it shows that Lambert Beer's law was followed. Parameters from the calibration curve is given below in table 4.5.

Table 4.5 UV absorbance

Absorbance	**Concentration**
0.931	20
0.829	18
0.757	16
0.676	14
0.562	12
0.454	10
0.361	8
0.242	6
0.196	4
0.106	2

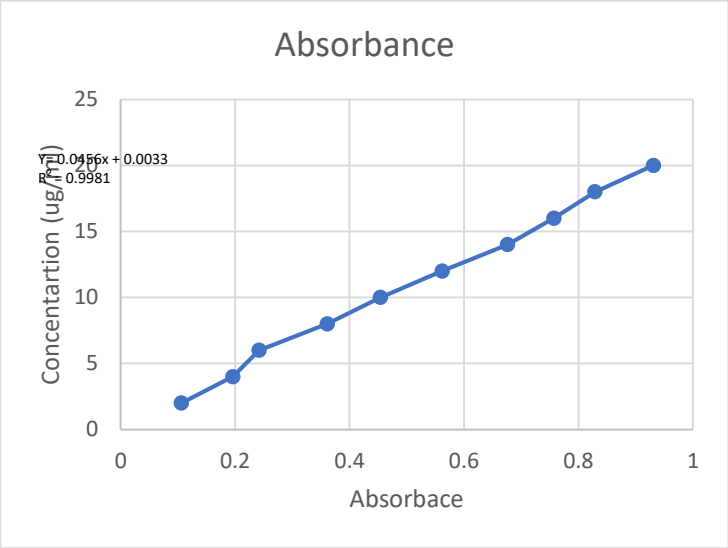

Figure 4.3 Rifampicin regressed curve at 337nm

4.2.3. sQBD Optimization by Box Behnken design

Quality-by-design, or QbD, is a critical process & product element way to optimize it produces the necessary CQAs formulation. The right design was chosen after considering a short phase in figuring out the factors interacted. Utilizing a BBD design with three components & three stages, the liposomal mix variables were optimized. A simple summary of the three independent variables is provided in fifteen preparation batches were made for RIF-TPGS-LIPO via a cast films method. Following a review of the response variable's acquired data, significant information was discovered that served as the statistical guideline for the study of statistics. The variables and different solutions were then examined in order to construct a quadratic polynomial model. The primary components' effects and potential interactions were described by ten distinct coefficients in total. The design's quadratic model was significant ($p<0.05$) based on the ANOVA findings. Table 1.6 is a list for the BBD study's findings.

Together with the several quadratic equations created for the response under investigation, VS, %EE, and PDI, results of the regression study of the one-way ANOVA variables are given. VS, % EE, and PDI. values of 0.9109, 0.9449, and 0.9380 for the Accepted Manuscript, respectively, indicating a substantially superior suitability of produced polynomials at $p\leq0.05$. Following the DoE data analysis, the 2D and 3D graphs were used to track and determine the important independent factors for that response. These charts show how each variable affects every response that the developed formulations are able to identify. Plots were scrutinized closely in order to determine the direct effects and inter-variable interactions that were important to take into account when selecting an experimental model. The magnitude of the independent variables predicted by the obtained equation for the model's validity analysis has been verified by creating an interim that was optimized using the layout space seen in the overlay plot.

Table no 4.6 Compile the different response & independent variables for each liposome formulation made in accordance with 3D Box-Behnken Design (BBD).

Type	Name	Unit	Change	Std.	Hight	Low
Factor	ST	Sec	Easy	0	1	-1
Response	VS	Nm		75.42	334.8	74.4
Response	% EE	%		12.35	91.34	49.82
Factor	TPGS		Easy	0	1	-1
Response	PDI			0.1727	0.322	0.085
Factor	CHOL: PC		Easy	0	1	-1

4.2.4. Surface morphology by TEM

Morphological characteristics of Rifampicin loaded liposomes was studied using transmission electron microscopy observed that optimised Rifampicin loaded liposomes confirmed that particle was spherical in shape with a well identified structured were visible. The particle size of RIF-TPGS-LIPO was found to be 144nm as shown in Fig. 1.4 Furthermore, TEM images showed that the uniform size of the liposomes.

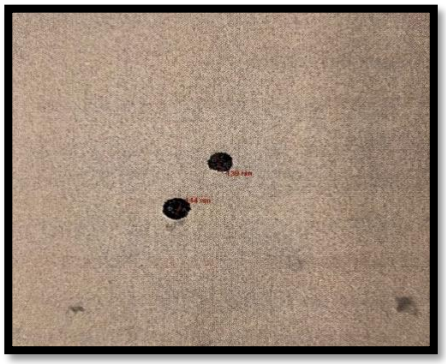

Figure 4.4 TEM image of optimized RIF-TPGS-LIPO

4.2.5. XRD Study

The crystalline-amorphous state of materials may be determined via X-ray diffraction. Fig. 4.5 displays the XRD spectra of the both lyophilized RIF-LIPO and RIF-TPGS-LIPO. In general, crystalline materials exhibit a series of sharp peaks, whereas amorphous materials have wide, undefined peaks. The characteristics diffraction pattern of RIF reveals sharp crystalline peaks at various 20 angles. Sharp peaks were seen in the XRD patterns of RIF with dispersed angles ranging from 20° to 30° (fig.4.5). While, RIF-LIPO displays a typical amorphous pattern as would be expected for a random polymerization result, free RIF displays distinct peaks in the diffractogram that indicate the presence of a crystalline phase in its natural form.

When compared to the free drug, the XRD pattern of RIF-TPGS-LIPO shows fewer and weaker peaks, as well as the disappearance of sharp peaks, which further suggests that Rifampicin has changed phases from crystalline to amorphous. Likewise, the data gathered from DSC analyses on RIF-LIPO, and RIF-TPGS-LIPO.

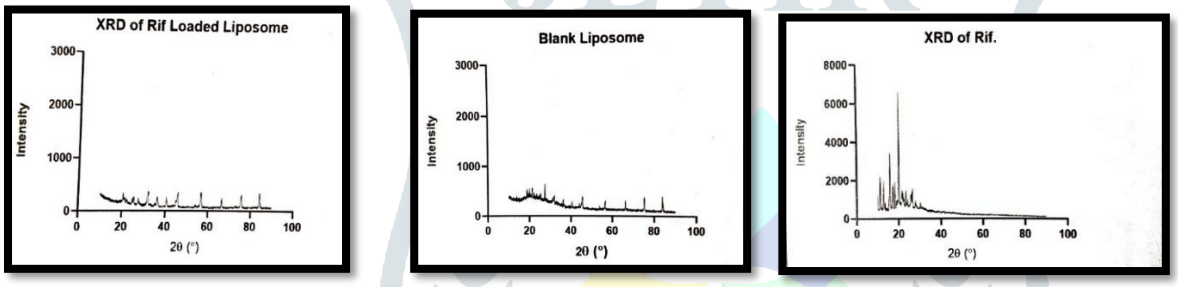

Figure 4.5 XRD spectra of RIF, Blank LIPO, & RIF- TPGS-LIPO

4.2.6. DSC Study

Differential scanning calorimetry (DSC) was performed using a DSC 6000, PerkinElmer, that was calibrated with indium. Three to five milligrams of PC, CHOL, RIF, TPGS, RIF-LIPO, or RIF-LIPO-TPGS were employed in the analysis. RIF exhibits a solid-liquid phase transition between 180°C and 185°C, according to results from the DSC thermogram and RIF-TPGS-LIPO, determining its melting point the exothermic peak at 260°C is related to the destruction of Rifampicin as shown in Fig 4.6 (A) In the RIF-TPGS-LIPO formulation thermogram, Rifampicin endothermic peak at 165°C is obvious that confirms the presence of intact RIF in liposomal formulation Fig 4.6 (B).

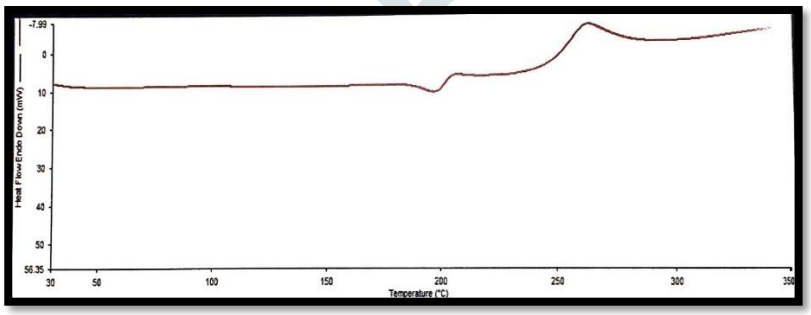

A)

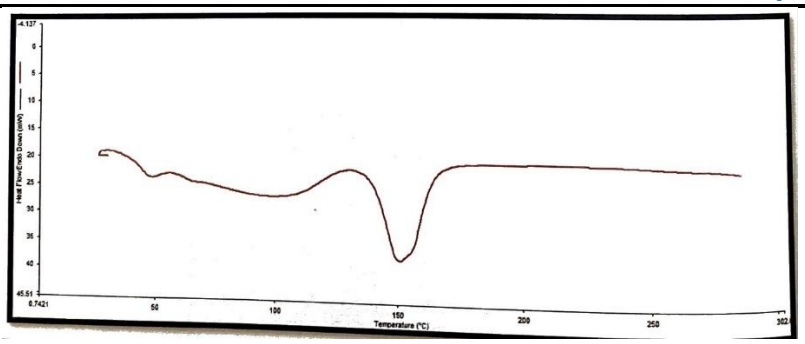

Figure 4.6 DSC Thermogram of A) Rifampicin B) TPGS Coated rifampicin liposomes

B)

4.3. In vitro drug release study

Utilizing a dialysis approach, we studied RIF releases kinetics in PBS as a diffusion fluid around 37.1°C to try to decipher that in-vitro RIF releasing behavior from RIF-LIPO and RIF-TPGS-LIPO vesicles. Over the course of 72 hours, the amount of release of liposomes packed by Rifampicin or liposomes that used It TPGS, or was investigated. Rifampicin TPGS liposomes demonstrated about 56+2.7% of the medication release in 72 hours, while more than 73+2.5% of Rifampicin was released in that time, as well, in Figure 4.7. The existence of TPGS Since these carriers were proven to be able to release the medication continuously The observed significant difference (p0.05) in drug release between RIF-TPGS-LIPO and RIF-LIPO could possibly be caused by a presence or TPGS at the outside of RIF-TPGS-LIPO. This might be explained by the possibility that the long alkyl chains of TPGS served like an inhibitor for the spread of RIF, so it was basically held inside TPGS-coated liposomes. This might lengthen the drug's period of action at the sick location and enhance its effectiveness against multi-drug-resistant bacteria.

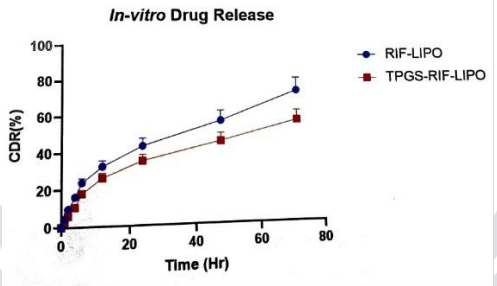

Figure 4.7 in- vitro release profile of RIF-LIPO suspension & RIF-TPGS-LIPO suspension in phosphate buffer (7.4pH)

4.4. Minimum Inhibitory Concentration (MIC):

Using Mueller-Hinton Broth, the MIC was calculated using the microdilution method. To obtain concentrations ranging from 0.025 to 50 g/ml, the formulations RIF, RIF-LIPO, and RIF-TPGS-LIPO were added to 96-well microplates and serially diluted. Three to five S. aureus colonies were dispersed into a saline solution from 18 to 24-hour agar cultures, and the bacterial inoculum was adjusted using a spectrophotometer (337 mm, OD 0.1, 1 to 2 108 CFU/ml). MIC values observed for RIF, RIF-LIPO, RIF-TPGS-LIPO against streptococcus aureus strains (ATCC 29213) tested separately. MIC value for RIF is 0.48 (g/ml), growth inhibition 50% GIso is 0.76 (ug/ml) and growth inhibition 90% Glo (ug/ml). whereas the MIC Value of RIF-LIPO is 0.35 (ug/ml), GIso is 0.59 (ug/ml) and GIg is 1.29. MIC value for RIF-TPGS-LIPO is 0.21 (ug/ml), GIso is 0.47 (ug/ml) GIg is 0.85(g/ml) as shown in table 4.7. hence the inhibitory concentration effect of RIF-TPGS-LIPO is lower than RIF and RIF-LIPO as shown in Fig 4.8

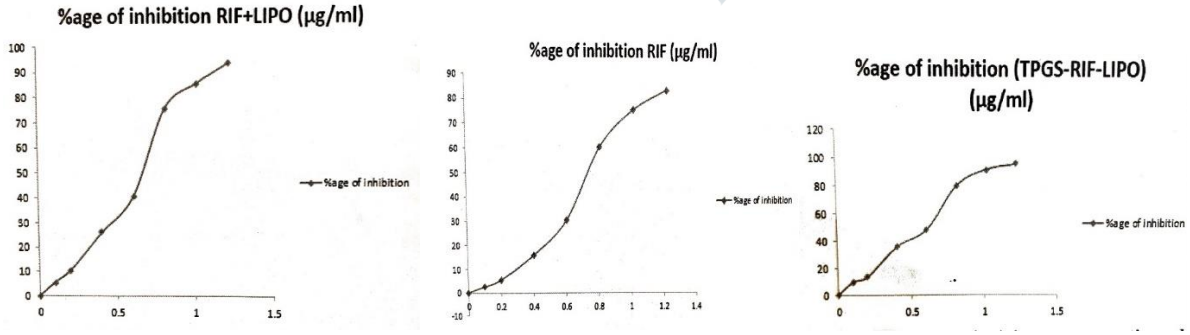

Figure 4.8 Minimum inhibitory concentration value graph of RIF, RIF-LIPO, RIF-TPGS-LIPO with growth inhibition 50 & growth inhibition 90

Table no. 4.7 MIC, GI50 & GI90 values of different formulation against S. aureus (ATCC 29213) bacterial cell.

Sample	GI_{90} (µg/ml)	GI_{50} (µg/ml)	MIC (µg/ml)
RIF-TPGS-LIPO	0.85	0.47	0.21
RIF-LIPO	1.29	0.59	0.35

RIF	1.52	0.76	0.48

4.5. ROS detection by flow cytometry

ROS generation was determined by the FACS study using 2', 7'-Dichlorofluorescin diacetate (DCFDA). A significantly higher level of ROS was observed in S. aureus strain (ATCC 29213) exposed to RIF-TPGS-LIPO in comparison with RIF-LIPO and free RIF (fig 4.9). The MFI value of control, free RIF, RIF-LIPO and RIF-TPGS-LIPO has found to be 3170, 3417, 5957 and 11942 respectively as shown in table 4.8. In connection to previous MIC result, it could be concluded that the result suggested that in S. aureus (ATCC 29213) cells, RIF-TPGS-LIPO significantly increased cytotoxicity by increasing ROS activity ($p<0.001$).

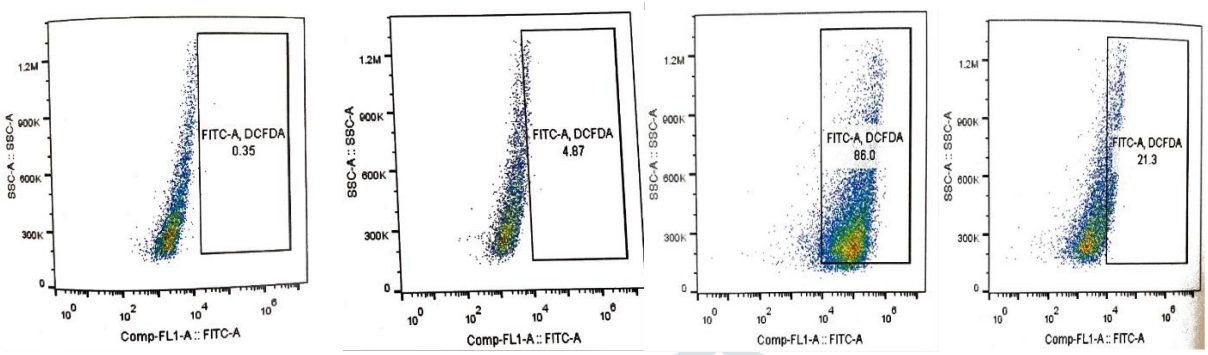

Figure 4.9 ROS Detection by flow cytometry of Control, RIF, RIF-LIPO, RIF- TPGS- LIPO

Table no. 4.8 Mean Fluorescence intensity (MFI) By flow cytometry for ROS detection

Sample	MFI
Control	3170
RIF (0.3ug/ml)	3417
RIF- LIPO (0.3 ug/ml)	5957
RIF-TPGS-LIPO (0.3 ug/ml)	11942

4.6. Cellular uptake determination by flow cytometry

Rapid flow cytometry was used to test the vitality of MRSA cells. This study focused on the formulations of free RIF, RIF-LIPO, and RIF-TPGS-LIPO, which were shown to be the most promising formulations when compared to free RIF and other formulations from the In vitro antibacterial activity investigation. A PI mean fluorescence intensity was seen following the administration of free RIF, RIF-LIPO, and RIF-TPGS-LIPO to the MRSA cells (fig 4.10). At their respective MICs (1.56 g/ml, 1.56 g/ml, and 1.56 g/m.), Control, RIF, RIF-LIPO, and RIF-TPGS-LIPO displayed 1244, 1253, 1295, and 27228 as shown in table 4.9 These findings confirm the In vitro antibacterial activity results from the preceding section, demonstrating the superiority of the RIF-TPGS-LIPO in terms of enhancing the antibacterial activity of free RIF and RIF-LIPO.

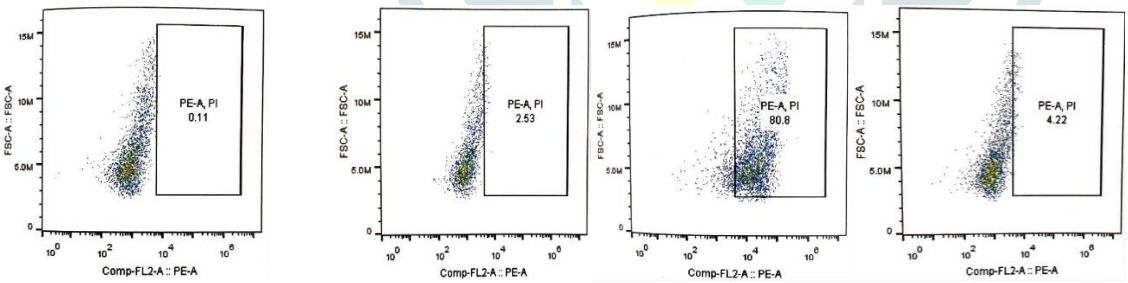

Figure 4.10. Bacterial cell viability by flow cytometry of control, RIF, RIF- LIPO & RIF -TPGS-LIPO

Table no.4.9 Mean Fluorescence intensity (MFI) by flow cytometry for bacterial cell viability

Sample	MFI
Control	1244
RIF (0.3ug/ml)	1253
RIF- LIPO (0.3 ug/ml)	1295
RIF-TPGS-LIPO (0.3 ug/ml)	27228

Conclusion:

The resistance of bacteria to first-line antibiotics, such as RIF, has emerged as a significant worldwide public health issue. In order to overcome this problem, other treatment techniques have been proposed, like concentrate dosing Approved Manuscript. RIF loaded liposomes based on TPGS were developed in this work to deliver RIF to the disease site in a focused & prolonged manner. Improvements made by BBD to the use of TPGS, or as additives for liposomal gels may prove helpful the creation of various tailored liposomal formulations intended to deliver antibacterial drugs.

The RIF administration via TPGS-based liposomes might be an exciting drug transport method for antibiotics in order to prevent resistance, related adverse effects, and possible enhancement. The QD technique could be a unique tool for liposome formulation optimization, as this example shows. It was also helpful understanding how process factors influenced desired important qualities (such VS, ZP, %EE, and PDI). The developed formulation may be useful reducing the RIF dosage and dosing frequency.

Acknowledgement: I am privileged to express my sincere gratitude to our principal sir for providing us the opportunity to write this research article under the guidance and support of **Mrs**. **Santoshi shah** and **Dr. Shrivanand patil** also my institute Shri dev Bhoomi institute of education science & technology for kind support and encouragement.

References:

1. Bhalani, D. V, Nutan, B., Kumar, A., & Singh Chandel, A. K. (2022). Bioavailability enhancement techniques for poorly aqueous soluble drugs and therapeutics. *Biomedicines*, *10*(9), 2055.
2. Cao, Z., Liu, Y., & Zhao, J. (2014). Efficient discrimination of some moss species by fourier transform infrared spectroscopy and chemometrics. *Journal of Spectroscopy*, *2014*.
3. Cegielski, J. P., Tudor, C., Volchenkov, G. V, & Jensen, P. A. (2021). Antimicrobial drug resistance and infection prevention/control: Lessons from tuberculosis. *International Journal of Infection Control*, *17*.
4. Chooi, K. Y., Comerford, A., Sherwin, S. J., & Weinberg, P. D. (2016). Intimal and medial contributions to the hydraulic resistance of the arterial wall at different pressures: a combined computational and experimental study. *Journal of The Royal Society Interface*, *13*(119), 20160234.
5. Dadgostar, P. (2019). Antimicrobial resistance: implications and costs. *Infection and Drug Resistance*, 3903–3910.
6. Gao, Y., Zuo, J., Bou-Chacra, N., Pinto, T. de J. A., Clas, S.-D., Walker, R. B., & Löbenberg, R. (2013). In vitro release kinetics of antituberculosis drugs from nanoparticles assessed using a modified dissolution apparatus. *BioMed Research International*, *2013*.
7. Gill, P., Moghadam, T. T., & Ranjbar, B. (2010). Differential scanning calorimetry techniques: applications in biology and nanoscience. *Journal of Biomolecular Techniques: JBT*, *21*(4), 167.
8. Jain, R. L., & Shastri, J. P. (2011). Study of ocular drug delivery system using drug-loaded liposomes. *International Journal of Pharmaceutical Investigation*, *1*(1), 35.
9. Jones, T. M. (2018). *Preformulation studies*.
10. Kurmi, B. Das, & Paliwal, S. R. (2022). Development and optimization of TPGS-based stealth liposome of doxorubicin using Box–Behnken design: characterization, hemocompatibility, and cytotoxicity evaluation in breast cancer cells. *Journal of Liposome Research*, *32*(2), 129–145.
11. Lai, Y. W., Kemsley, E. K., & Wilson, R. H. (1994). Potential of Fourier transform infrared spectroscopy for the authentication of vegetable oils. *Journal of Agricultural and Food Chemistry*, *42*(5), 1154–1159.
12. Lee, S. M., man Kim, J., Jeong, J., Park, Y. K., Bai, G.-H., Lee, E. Y., Lee, M. K., & Chang, C. L. (2007). Evaluation of the broth microdilution method using 2, 3-diphenyl-5-thienyl-(2)-tetrazolium chloride for rapidly growing mycobacteria susceptibility testing. *Journal of Korean Medical Science*, *22*(5), 784.
13. Maha, A. H., & AS, A.-D. E. (2020). HYDROPHOBIC ION-PAIRED DRUG DELIVERY SYSTEM: A REVIEW. *Indian Drugs*, *57*(1).
14. Majumder, M. A. A., Rahman, S., Cohall, D., Bharatha, A., Singh, K., Haque, M., & Gittens-St Hilaire, M. (2020). Antimicrobial stewardship: Fighting antimicrobial resistance and protecting global public health. *Infection and Drug Resistance*, 4713–4738.
15. Morel, C. M., Alm, R. A., Årdal, C., Bandera, A., Bruno, G. M., Carrara, E., Colombo, G. L., de Kraker, M. E. A., Essack, S., & Frost, I. (2020). A one health framework to estimate the cost of antimicrobial resistance. *Antimicrobial Resistance & Infection Control*, *9*, 1–14.
16. Musielak, E., Feliczak-Guzik, A., & Nowak, I. (2022). Optimization of the conditions of solid lipid nanoparticles (SLN) synthesis. *Molecules*, *27*(7), 2202.
17. Ranjalkar, J., & Chandy, S. J. (2019). India's National Action Plan for antimicrobial resistance–An overview of the context, status, and way ahead. *Journal of Family Medicine and Primary Care*, *8*(6), 1828–1834.
18. Salam, M. A., Al-Amin, M. Y., Salam, M. T., Pawar, J. S., Akhter, N., Rabaan, A. A., & Alqumber, M. A. A. (2023). Antimicrobial resistance: a growing serious threat for global public health. *Healthcare*, *11*(13), 1946.
19. Singh, D., Agusti, A., Anzueto, A., Barnes, P. J., Bourbeau, J., Celli, B. R., Criner, G. J., Frith, P., Halpin, D. M. G., & Han, M. (2019). Global strategy for the diagnosis, management, and prevention of chronic obstructive lung disease: the GOLD science committee report 2019. *European Respiratory Journal*, *53*(5).
20. Sun, Y.-S., Zhao, Z., Yang, Z.-N., Xu, F., Lu, H.-J., Zhu, Z.-Y., Shi, W., Jiang, J., Yao, P.-P., & Zhu, H.-P. (2017). Risk factors and preventions of breast cancer. *International Journal of Biological Sciences*, *13*(11), 1387.
21. Tang, X., Zhao, Y., Yu, H., Cui, S., Temple, H., Amador, E., Gao, Y., Chen, M., Wang, S., & Hu, Z. (2023). Concentration-regulated multi-color fluorescent carbon dots for the detection of rifampicin, morin and Al3+. *Materials Today Advances*, *18*, 100383.
22. Uchil, R. R., Kohli, G. S., KateKhaye, V. M., & Swami, O. C. (2014). Strategies to combat antimicrobial resistance. *Journal of Clinical and Diagnostic Research: JCDR*, *8*(7), ME01.
23. Ventola, C. L. (2015). The antibiotic resistance crisis: part 1: causes and threats. *Pharmacy and Therapeutics*, *40*(4), 277.
24. Walvekar, P., Gannimani, R., Salih, M., Makhathini, S., Mocktar, C., & Govender, T. (2019). Self-assembled oleylamine grafted

hyaluronic acid polymersomes for delivery of vancomycin against methicillin resistant Staphylococcus aureus (MRSA). *Colloids and Surfaces B: Biointerfaces*, *182*, 110388.

25. Zhu, T. F., Budin, I., & Szostak, J. W. (2013). Preparation of fatty acid or phospholipid vesicles by thin-film rehydration. *Methods in Enzymology*, *533*, 267–274.